Energy Separation Algorithms Applied to Sonar Data

R.K. Lennartsson[1], S. McLaughlin[2], M.J. Levonen[1], J.W.C. Robinson[1] and L. Persson[1]
[1]Swedish Defence Research Agency, SE-17290 Stockholm, Sweden
[2] Institute for Digital Communication, School of Engineering and Electronics
University of Edinburgh,Edinburgh, EH9 3JL, UK.

Abstract

Energy separation algorithms (ESA) using Teagers energy operator have been used to analyze modulations in speech resonances, energy separation in bird song and in the resynthesis of musical instrument sounds. The data set used in the analysis here is from a sea trial in the Baltic sea. A 23ft fiberglass boat was equipped with accelerometers for source signal recordings from the engine and the hull. The sound propagated through the water was picked up with a passive hydrophone array. The analysis of the accelerometer data was used to identify frequencies associated with engine and propeller rotation. Frequency components not harmonically related to either the engine crank shaft or drive were identified in the hydrophone data. The ESA was then applied to the none related frequencies. It is shown that ESA can be used as a tool to identify stability and time dependency of frequencies.

I. Introduction

In sonar signal processing identification and classification of different underwater sources are crucial. In passive sonar analysis the estimation problems are often focused on spectral separation and characterization of the narrow-band signals emitted from different parts of the target, e.g. engine, drive and hull. In many times the power spectrum is able to separate these sources. If a more precise description of targets is required the relation and coupling between frequencies may need to be uncovered. One possible way to do this is by using higher-order spectra, e.g. [1]. From the bispectrum the phase coupling patterns can be obtained and thereby be used as a tool for association of different physical mechanisms such as engine and drive. In all spectral analysis it is important to use as significant spectral values as possible for source parameter estimation. In spectral analysis second-order stationarity is normally assumed, at least within the observation window. The estimated spectra may be erroneous if the data contains disturbances and transients. In this paper use is made of Teagers Energy operator as proposed by Maragos and his co-workers [2, 3, 4] to determine the stability of the power spectral peaks. The data is from a sea trial conducted in a shallow bay in the Baltic Sea off the east coast of Sweden. The water depth at the site was approximately 30 m. The trials were performed using a 23-ft. fiberglass motor boat with a 4-cyl. 4-stroke, turbo-charged diesel engine as sound source. The boat was equipped with accelerometers for source signal recordings. We allowed the boat run on straight tracks from far distance with a constant speed and approaching and passing an array of bottom mounted hydrophones. Engine and hull vibrations were recorded with accelerometers fitted directly on the hull and the engine. The radiated sound in the water was recorded by bottom-mounted wide-band hydrophones. The sampling rate was 25 kHz for all recording channels. Ambient sea noise was recorded before and after the sea trial. The weather conditions were good throughout the whole experiment with a wind speed below 5 m/s.

Previously [1] bispectral analysis was used to assess the level of quadratic coupling present in the dataset discussed above. However, it was difficult to discern precisely the level of coupling because much of the coupling lay between harmonics of the generating signals which were themselves phase coupled by the stiff mechanism in the engine/drive gear assembly. This paper reports an analysis of the frequency content of the data, in particular frequency components not harmonically related to either the rotation of the engine crank shaft or drive (gear box and propeller) were identified. In the work presented here we use the ESA to assess the level of stationarity and stability of the unrelated frequency components in the original data set. The aim is to use this assessment at a later date to select particular segments for an analysis by bicoherence.

II. Energy Separation

The use of the Teager Energy operator to separate the amplitude and frequency modulated (AM/FM) components of mixed signals with AM and FM components. Much of the early work to elucidate the properties of this operator was performed by Maragos and his co-workers [2, 3]. For example, for discrete-time signals the energy operator is given by,

$$\Psi_d[x(n)] \;=\; x^2(n) - x(n+1)x(n-1) \qquad (1)$$

which can be used to find the amplitude and frequency of signals of the form,

$$x(n) \;=\; A\cos(\Omega_c n \;+\; \theta). \qquad (2)$$

The energy operator is applied to both the signal and the first difference, given by

$$y(n) \;=\; x(n) - x(n-1). \qquad (3)$$

The instantaneous amplitude and frequency can be obtained from,

$$\Omega_c \;=\; \arccos\left(1 - \frac{\Psi[y(n)]}{2\Psi[x(n)]}\right) \qquad (4)$$

and

$$|A| \;=\; \sqrt{\frac{\Psi[x(n)]}{sin^2(\Omega_c)}}. \qquad (5)$$

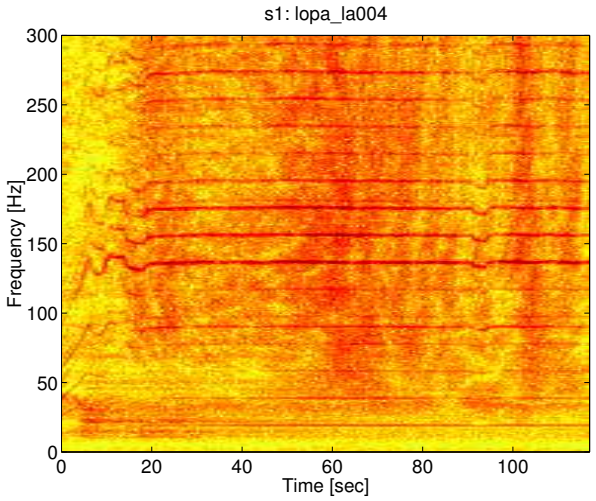

Figure 1: Spectrum of frequency range 0 to 300 Hz for engine accelerometer with the boat moving

III. Results and Analysis

An extensive analysis of the data set was carried out considering the power spectra, short-time fourier transform (STFT) and finally ESA was applied to the frequency components which appeared to be not harmonically related to any rotating elements. In Fig. 1 the STFT is displayed. In this case the boat is moving with the engine running at approximately 3000rpm (actually 2712rpm) with the drive connected. The frequencies are varying a lot during the first 20 seconds. The reason is that the recording is started when the boat was standing still and that it takes some time for the boat to reach a stable speed with a fixed rpm. For the rest of the run the frequencies are quite stable except for the 90 to 95 [sec] section (the rpm was shortly lowered by the driver).

In Fig.2 the output of ESA applied to the strongest component identified in the STFT of the hydrophone data (136.7 Hz later found to be the rotation frequency of the propeller shaft modulated by the number of propeller blades) is displayed. The ESA shows the same over all picture as the STFT but in greater detail, especially for the amplitude. The frequency is very stable (except for the time segments mentioned above) but the amplitude shows some variance.

For the rest of the analysis the data was considered as three distinct data sets divided as follows:

- **Block 1:** The engine running at 3000rpm with the boat moving (25-40 seconds)
- **Block 2:** The engine running at 3000rpm with the boat moving (65-80 seconds)
- **Block 3:** The engine running at 3000rpm with the boat moving (100-115 seconds)

The distinction between the three blocks relates to the position of the boat with relation to the hydrophone array. In block 1 the boat is far away and approaching, block 2 contains the closest point of approach and in block 3 the boat is moving away from the array. The data analyzed here includes hydrophone data and data from an engine mounted accelerometer.

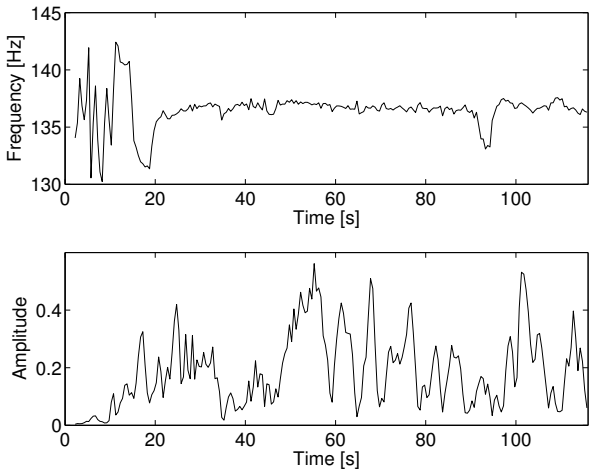

Figure 2: Results of ESA analysis at frequency component at 136.7 Hz in hydrophone data (in Block 1).

A. Block 1

In this sub-section the data in block 1 is analyzed with power spectrum and ESA. In block 1 the boat is far away from the hydrophone and slowly approaching it. The spectra were generated using Matlab with a 65536 point FFT resulting in a frequency resolution of approximately 0.4 Hz.

The power spectrum of both the hydrophone (see Fig. 3 and 4) and accelerometer (see Fig. 5 and 6) data contains strong peaks for frequencies up to 600 Hz. All strong peaks have been identified and these are indicated in the Figures.

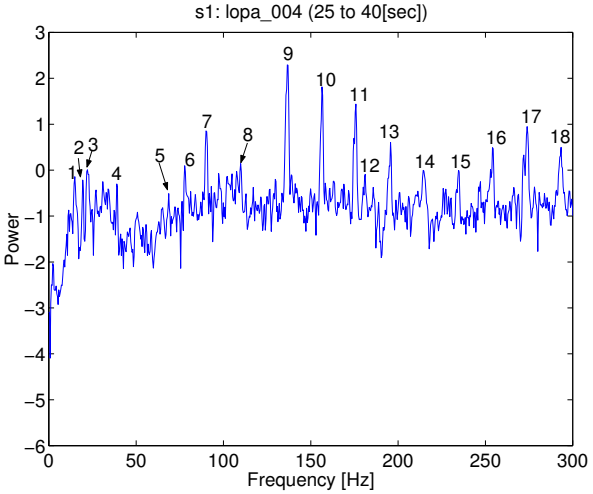

Figure 3: Spectrum of frequency range 0 to 300 Hz for the hydrophone data in Block 1.

In addition, all identified peaks were tabulated in three tables (not shown here) which indicate the following:

- The frequency peaks that are related to the rotation of the engine axes
- The frequency peaks related to the propeller shaft
- The frequency peaks that are not related to anyone of the previously mentioned frequencies in the other

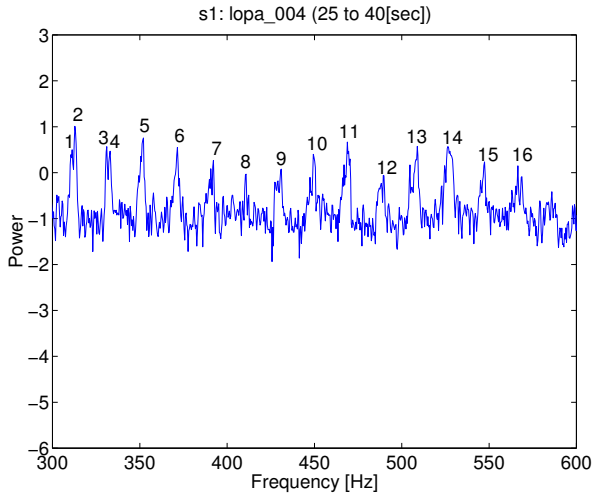

Figure 4: Spectrum of frequency range 300 to 600 Hz for the hydrophone data in Block 1.

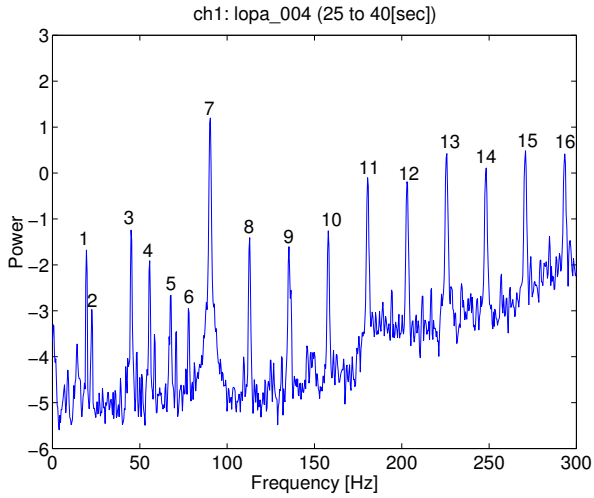

Figure 5: Spectrum of frequency range 0 to 300 Hz for the engine accelerometer data in Block 1.

tables

From the analysis of these spectra and others not illustrated here it is apparent that many of the peaks are multiples of 22.6 Hz, which corresponds to one half of the rotation frequency of the engine axes. In addition there are multiples of 19.5 Hz which corresponds to the frequency of rotation of the propeller shaft. The gear ratio between the propeller shaft and the engine axes is 2.31. If these frequencies are discounted the frequencies which are not related to either of these are only found in the hydrophone data. Discounting very low frequencies where the SNR was low, the following frequency peaks were found 109.9 Hz, 333 Hz, 392.1 Hz, 431 Hz, 489.6 Hz and 508.9 Hz.

The ESA was then applied to each of the unrelated frequencies. In Fig. 7 to 12 the output of the ESA is displayed. In the upper panel the ESA estimated frequency is displayed and in the lower panel the amplitude is shown. The most stable components are 333 Hz, 489.6 Hz, 508.9 Hz, while the 109.9 Hz peak shows the largest variance. The variations in amplitude can be explained by multipath propagation of the sound waves. The site is very shallow

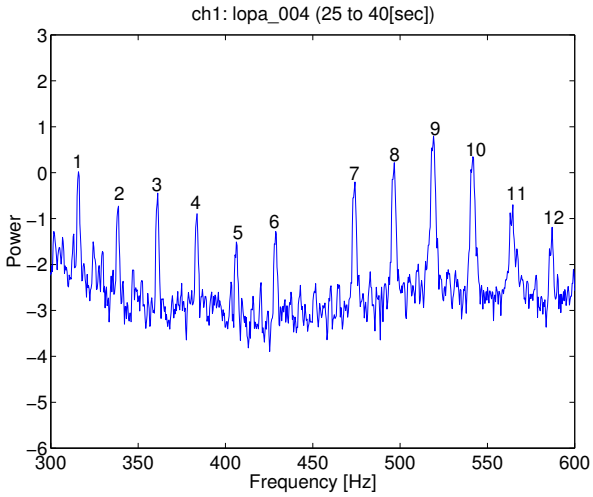

Figure 6: Spectrum of frequency range 300 to 600 Hz for the engine accelerometer data in Block 1.

and the sound source remains at fairly constant frequencies so the influence from earlier and later arrivals (surface and sea-floor reflections) interferes with main propagation path giving the varying amplitude that can be seen in the figures mentioned above.

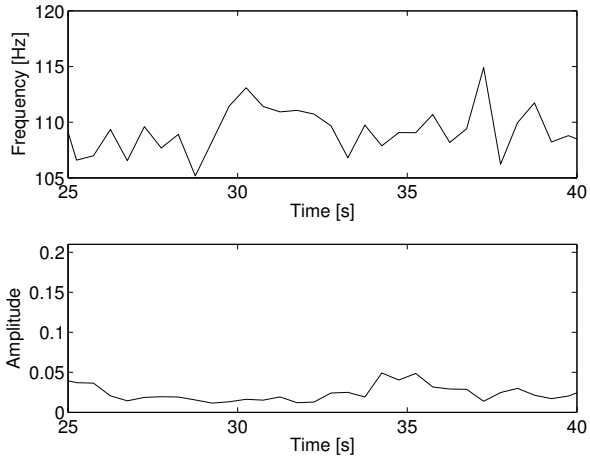

Figure 7: Results of ESA analysis at frequency component at 109.9 Hz in hydrophone data (in Block 1).

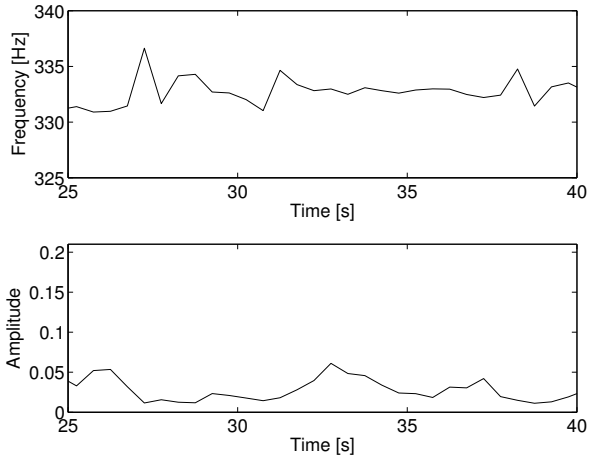

Figure 8: Results of ESA analysis at frequency component at 333 Hz in hydrophone data (in Block 1).

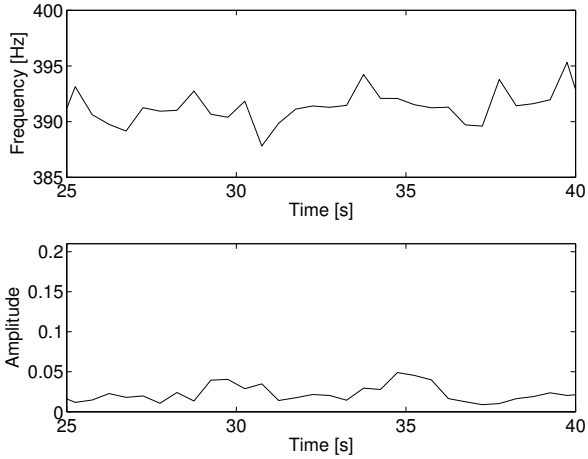

Figure 9: Results of ESA analysis at frequency component at 392.1 Hz in hydrophone data (in Block 1).

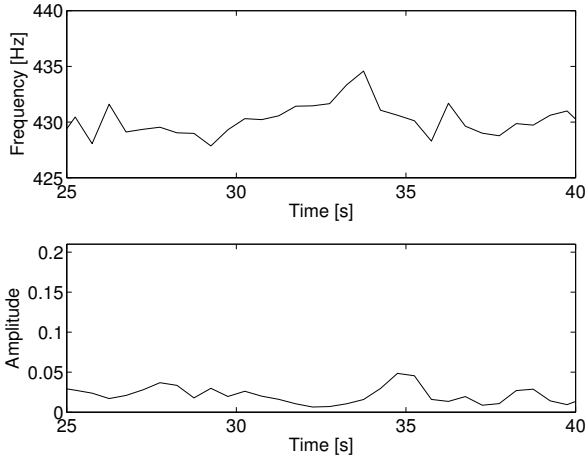

Figure 10: Results of ESA analysis at frequency component at 431 Hz in hydrophone data (in Block 1).

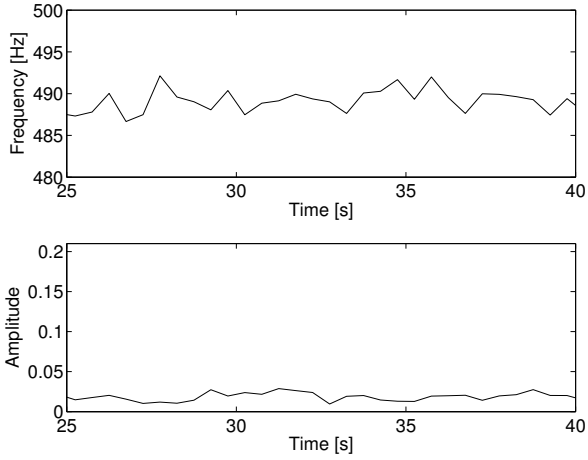

Figure 11: Results of ESA analysis at frequency component at 489.6 Hz in hydrophone data (in Block 1).

B. Block 2

In this sub-section data from Block 2 is analyzed. The boat moving towards and passing over the hydrophone.

Following the same procedure as for Block 1 (the spectra are not shown here) and discounting those frequencies associated with the mechanical vibrations results in identifying the remaining frequencies. Interestingly only one frequency was identified in the hydrophone data at 64.5 Hz. In Fig. 13 the output of the ESA is displayed. The amplitude is quite stable while the frequency shows some variance.

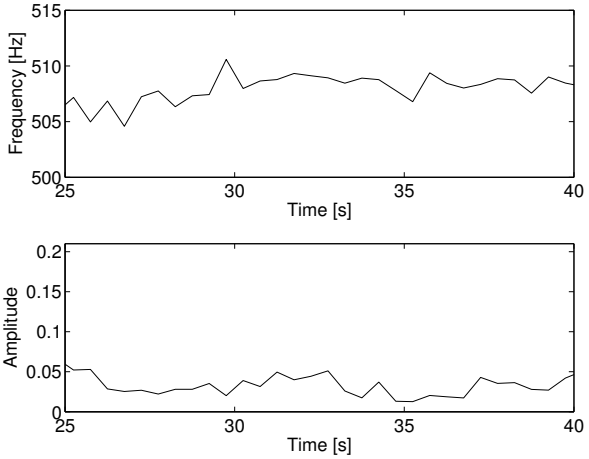

Figure 12: Results of ESA analysis at frequency component at 508.9 Hz in hydrophone data (in Block 1).

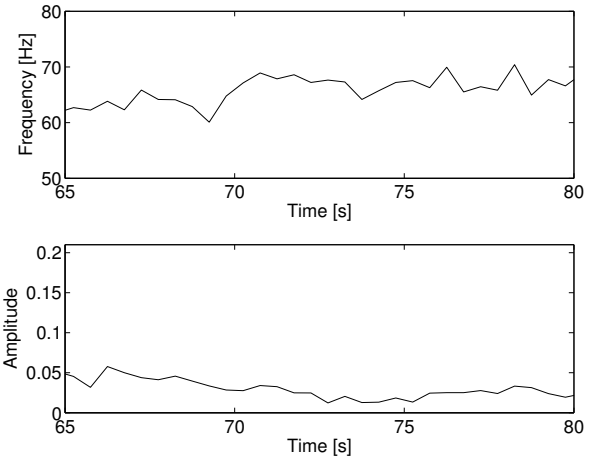

Figure 13: Results of ESA analysis at frequency component at 64.5 Hz in hydrophone data (in Block 2)

C. Block 3

In this sub-section the data in Block 3 is analyzed, here the boat is moving away from the hydrophone.

Following the same procedure as for Blocks 1 and 2 and discounting those frequencies associated with the mechanical vibrations results in identifying the remaining frequencies. In this case two frequencies were identified in the hydrophone data at 469.6 Hz and 538.6 Hz. In Fig. 14 to 15 the output of the ESA is displayed. The 469.6 Hz is quite stable in both amplitude and frequency, while the 538.6 Hz peak shows quite large variance in frequency.

IV. Conclusions

This paper has presented some preliminary analysis of a sonar data set which has been analyzed previously using normalized bispectrum. The ESA gives a more detailed picture of the frequency and amplitude variations than the spectrum or the STFT (for one frequency component at a time). The ESA results shown indicate some consistency

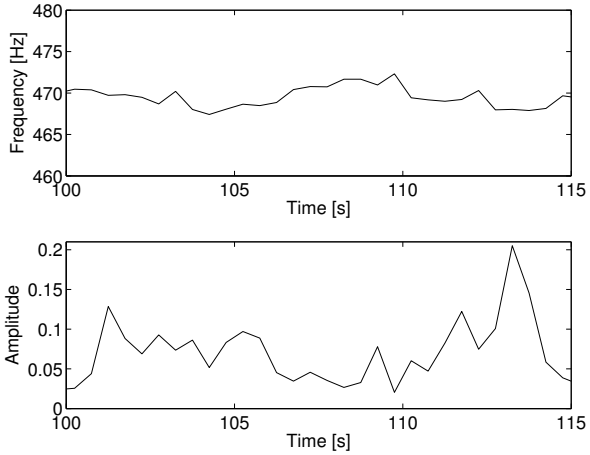

Figure 14: Results of ESA analysis at frequency component at 469.6 Hz in hydrophone data (in Block 3).

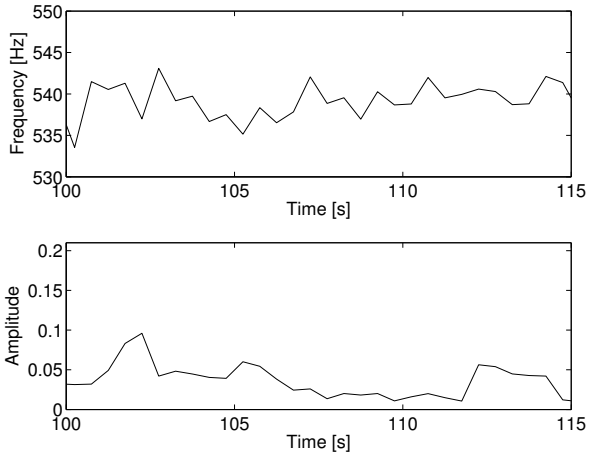

Figure 15: Results of ESA analysis at frequency component at 538.6 Hz in hydrophone data (in Block 3).

in the unrelated frequency components and help identify areas where the components are likely to be strongest. The source of the unrelated frequencies are not known to us, but most likely they are generated by some rotating mechanism (other than engine crank shaft or drive) on the boat. The analysis presented here has indicated that in order to perform the data analysis using normalized bispectrum it is necessary to identify those segments where stationarity is strongest and few transients exist. The ESA has enabled this and can hence be a useful tool in the analysis of sonar data.

V. REFERENCES

[1] R.K. Lennartsson, L. Persson, J.W.C. Robinson and S. McLaughlin, "Passive signature characterization by bispectral analysis," *Proc. IEEE Nordic Signal Processing Symposium, NORSIG 2000,* Kolmarden, Sweden, June 2000, pp. 445–448.

[2] B. Santhanam and P. Maragos, "Energy demodulation of two component am-fm signal mixtures," *IEEE Signal Processing Letters, vol. 3,* pp. 294–298, November 1996.

[3] P. Maragos, J. Kaiser and T. Quateri, "Energy separation in signal modulations with application to speech analysis," *IEEE Trans. Signal Processing,* pp. 3024–3051, October 1993.

[4] P. Maragos, J. Kaiser and T. Quateri, "On amplitude and frequency demodulation using energy operators," *IEEE Trans. Signal Processing,* pp. 1532–1550, April 1993.